much-used Kopal-computed values, as plotted in Ref 3, share this limitation with us

References

[1] Simon, W E and Walter, L A "Approximations for supersonic flow over cones," AIAA J 1, 1696–1698 (1963)

[2] Zumwalt, G W and Tang, H H "Mach number independence of the conical shock pressure coefficient," AIAA J 1, 2389–2391 (1963)

[3] "Equations, tables, and charts for compressible flow," Ames Res Lab , NACA Rept 1135, p 48 (1953)

Reply by Author to R E Lavender

A P Cappelli*
North American Aviation, Inc , Downey, Calif

An analytical procedure was outlined in Ref 1 for describing the touchdown dynamics of a lunar spacecraft The motion of the vehicle was defined by the classical Eulerian equations of rigid body motion

The application of external forces to the vehicle is determined by two controls incorporated in the digital computer program These two conditions require that a vehicle leg tip be in contact with the lunar surface and also have a resultant lateral or (positive) vertical velocity The velocities are referred to the body frame of reference When both conditions hold, forces equal to the crushing forces of the inelastic energy absorbers are applied to the leg tips The motion of each crushed leg tip is traced, and its relative position to the lunar surface is determined The deformation function described in Ref 1 is used to ascertain this relationship for each leg A positive or zero value of the function indicates surface contact for the respective vehicle legs Any implication of leg liftoff is determined from the actual trace of the leg-tip position and not from leg crushing rates However, the amount of permanent deformation of the vertical energy absorber can be determined from the deformation function

The activation of the lateral and vertical energy absorbers occurs independently For example, if the lateral leg-tip velocity is reduced to zero, the lateral force applied to that leg is zero This does not restrict activation of the vertical energy absorber if the leg tip still has vertical velocity When both vertical and lateral tip velocities vanish, the forces are removed and the vehicle undergoes rigid body motion provided the other legs are not in the process of crushing Realistically, since a step-by-step integration procedure is used, the velocities will most likely not vanish identically The small residual velocities that exist will induce external forces However, the force applications will be such as to approximate the true leg positions within the requirements dictated by the surface friction coefficient The end result will be that the time average of load applications will approximate the actual load history The smaller the time increments considered the better the approximation

As Lavender has correctly pointed out, forces of reduced magnitude are actually applied to the vehicle when the tip velocities vanish The writer was well aware of this condition when the problem was formulated three years ago It was decided at that time that for the inelastic energy absorbers under consideration the magnitude of the total impulse applied to the vehicle because of these reduced forces was

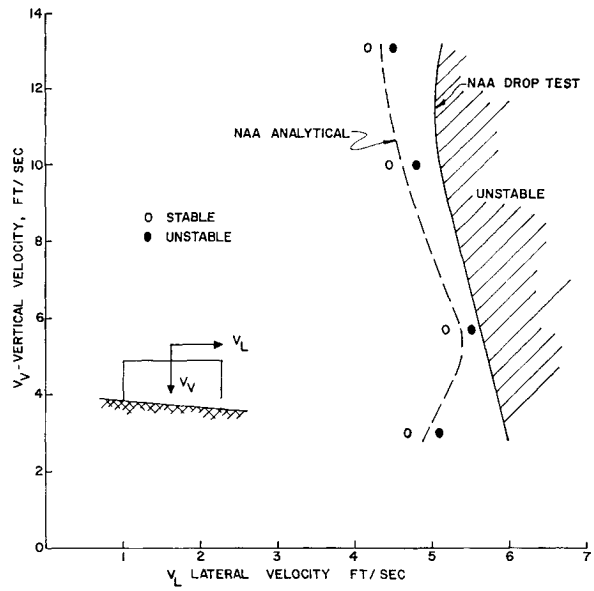

Fig 1 Lunar landing simulation test, North American Aviation Inc (Model data: R_1 = 1 55 ft; R_2 = 1 342 ft; R_3 = 0 775 ft; DCG = 1 555 ft; nF_V/m = 578 ft/sec²; I_y/m = 0.345 ft²; I_x/m = 0 345 ft²; coefficient of friction = 0 5; g = 32 2 ft/sec²; A = 5 ; B = 0 ; β = 270)

small compared to the crushing forces Correspondingly, the stability profile would not be seriously affected The basic program has since been modified by W D Brayton of the Space & Information Division to include the effects of reduced impact forces In cases run by Brayton, it was found that these forces are of little consequence and do not critically affect the stability profile The modified program has the added capability of considering the coefficient of friction, multistage landing systems, rotating landing gears, elasticity in the landing legs, and other refinements

The question of the validity of the outlined assumptions can only be answered by correlation with empirical evidence The outlined analytical procedure has been compared with the results of three independent drop test series to obtain this verification The first series of tests connected with the Surveyor program were outlined in Ref 1 Since publication of the paper, comparison has also been made with two other recent tests Figure 1 indicates the results of a series of 36 drop tests performed at the Space & Information Systems Division Development Laboratory The stability

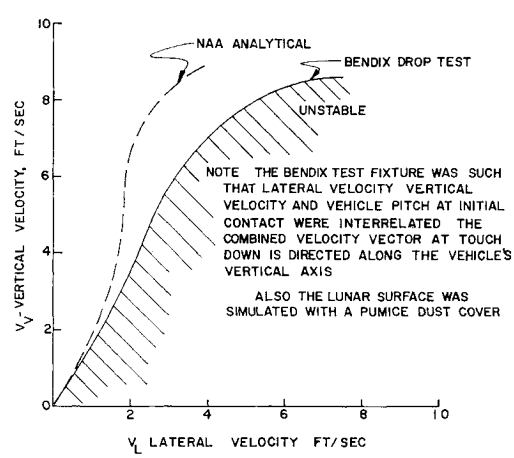

Fig 2 Lunar landing simulation test, Bendix Corp (Model data: R_1 = 1 212 ft; R_2 = 1 05 ft; R_3 = 0 607 ft; DCG = 1 506 ft; nF_V/m = 462 ft/sec²; I_x/m = 0 920 ft²; I_y/m = 0 920 ft²; I/m = 0 833 ft²; coefficient of friction = 0 5; g = 32 2 ft/sec²; A = 5°; B = 0 ; β = 270°)

Received November 12, 1963

* Specialist Research, Space and Information Systems Division

profile for tests conducted by Bendix Corporation[2] are shown in Fig 2 As can be seen from the figures, the analytical results agree favorably with experimental evidence It should be pointed out that in *no* instance were the analytical results *optimistic* as claimed by Lavender

The question of the discontinuity in the stability profile presented by the Marshall Space Flight Center computer program is of concern to the writer No such jump in the stability profile was obtained in the outlined analytical and experimental programs A continuous plot of the vehicle motion and impact force histories was obtained when the problem was formulated on the analog computer The results of this study are reported in Ref 3 The free-flight condition described by Lavender was obtained in both the digital and analog programs, but no discontinuity in the stability profile was observed It is unlikely that this condition explains the discontinuity in the Marshall Space Flight Center results Since the analytical procedure or mathematical model used are not described by Lavender, it is difficult to speculate as to the cause of the discontinuity

It should also be mentioned that the basic analysis was proposed for the consideration of the three-dimensional alightment problem

References

[1] Cappelli, A P , "Dynamics analysis for lunar alightment," AIAA J 1, 1119–1125 (1963)

[2] "Lunar landing module alighting gear" Rept *MM* 62 2, Bendix Corp , Bendix Products Aerospace Div (March 1962)

[3] Cappelli A P Parametric studies of the landing stability of lunar alightment vehicles," STR 79, Space & Information Div , North American Aviation, Inc (1961)

Some Effects of Planform Modification on the Skin Friction Drag

EDWARD J HOPKINS*
NASA Ames Research Center, Moffett Field, Calif

FOR the rapid estimation of the skin friction drag of airplane wing and control surfaces, it is sometimes the practice to use the Reynolds number based on the average chord of the surface in the calculations This note will show that, if a simple average geometric chord is used, such an approximate solution can differ significantly from the more exact solution involving a spanwise integration of the skin friction

The general planform of a half-wing to be analyzed is shown in Fig 1 with some of the symbols that will be used For a two-dimensional wing the average skin-friction coefficient can be represented by

$$C_F = K(R/l)^n c^n \tag{1}$$

where

n = exponent of skin-friction equation
K = constant of skin-friction equation (considered herein to include compressibility and heat-transfer effects)
R/l = unit Reynolds number

When the average skin friction obtained by Eq (1) at each spanwise station is integrated over the half-wing span s and the result is divided by the dynamic pressure and by the

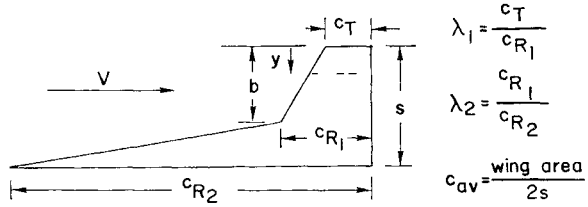

Fig 1 Geometry and symbols

plan area of the half-wing, we obtain a general expression for the skin-friction coefficient:

$$C_F = \frac{K(R/l)\,2^{n+1}(c_{av})^n}{n+2} \times \left\{\frac{\lambda_2}{(1+\lambda_2)[1-(b/s)] + (1+\lambda_1)(\lambda_2)(b/s)}\right\}^{n+1} \times \left\{\left[\frac{1-(\lambda_1)^{n+2}}{1-\lambda_1}\right]\frac{b}{s} + \left(1-\frac{b}{s}\right)\left[\frac{1-(\lambda_2)^{n+2}}{(1-\lambda_2)(\lambda_2)^{n+1}}\right]\right\} \tag{2}$$

for which the following limits apply:

$$0 \le \lambda_1 \le 1 \qquad 0 < \lambda_2 \le 1 \qquad 0 \le b/s < 1$$

where, by L'Hospital's rule,

$$\lim_{\lambda_1 \to 1}\left[\frac{1-(\lambda_1)^{n+2}}{1-\lambda_1}\right] = \lim_{\lambda_2 \to 1}\left[\frac{1-(\lambda_2)^{n+2}}{(1-\lambda_2)(\lambda_2)^{n+1}}\right] = n+2$$

When there are no restraints on the factors contained in Eq (2), the skin friction approaches 0 as $\lambda_2 \to 0$, obviously an impractical solution A family of planforms is analyzed, therefore, which contains wings having the same ratio of average chord to root chord To facilitate such an analysis, the notch ratio b/s in Eq (2) will be written as

$$\frac{b}{s} = \frac{1+\lambda_2-(2c_{av}/c_{R2})}{1-\lambda_1\lambda_2} \tag{3}$$

All wings will be assumed to be flying at the same unit Reynolds number and Mach number and to have the same average chord, span, and area If we consider only wings with $\lambda_1 = 0$, then from Eqs (2) and (3) we can write the equation of the skin-friction coefficient of the cranked wing to that for the untapered wing as

$$\frac{(C_F)_{\substack{\lambda_2 \\ \lambda_1=0}}}{(C_F)^{\lambda_1=\lambda_2=b/s=1}} = \frac{2^{n+1}}{n+2}\left(\frac{\lambda_2}{2c_{av}/c_{R_2}}\right)^{n+1}\left\{1+\lambda_2-\frac{2c_{av}}{c_{R_2}} + \left(\frac{2c_{av}}{c_{R_2}}-\lambda_2\right)\left[\frac{1-(\lambda_2)^{n+2}}{(1-\lambda_2)(\lambda_2)^{n+2}}\right]\right\} \tag{4}$$

The results of varying the inboard taper ratio λ_2 in Eq (4) on the skin friction of cranked wings to that for a rectangular wing are presented in Fig 2 for an assumed $2c_{av}/c_{R_2} = \frac{1}{2}$ for both the turbulent ($n = -\frac{1}{7}$ for large Reynolds numbers, see Ref 1) and the laminar ($n = -\frac{1}{2}$) boundary-layer cases Wing planforms are also shown in Fig 2 above each corresponding taper ratio For the conditions specified, it is apparent that using the average chord in calculating the skin friction of such planforms can lead to sizable errors

Wings having straight leading edges (no crank) will be considered next This case can easily be derived from Eq (2) by letting $b/s = \lambda_2 = 1.0$ Provided the same conditions are imposed on the tapered and the untapered wings, namely, that each wing has the same average chord, span, area, unit Reynolds numbers, and Mach number, then the skin-friction ratio for the tapered wing to that for the rectangular wing becomes

$$\frac{(C_F)_{\lambda_1}}{(C_F)_{\lambda_1=1}} = \frac{2^{n+1}}{n+2}\left(\frac{1}{1+\lambda_1}\right)^{n+1}\left[\frac{1-(\lambda_1)^{n+2}}{1-\lambda_1}\right] \tag{5}$$

Received November 15, 1963
* Research Scientist